Received: 26 February 2018 | Revised: 13 May 2018 | Accepted: 19 May 2018

DOI: 10.1002/jccs.201800073

JOURNAL OF THE CHINESE CHEMICAL SOCIETY

ARTICLE

A porous inorganic zirconyl pyrophosphate as an efficient catalyst for the catalytic transfer hydrogenation of ethyl levulinate to γ-valerolactone

Jianjia Wang[1] | Ruiying Wang[1] | Huimin Zi[1] | Haijun Wang[1] | Yongmei Xia[2] | Xiang Liu[1]

[1]Key Laboratory of Synthetic and Biological Colloids, Ministry of Education, School of Chemical and Material Engineering, Jiangnan University, Wuxi, Jiangsu, China

[2]State Key Laboratory of Food Science & Technology, Wuxi, Jiangsu, China

Correspondence
Haijun Wang, Key Laboratory of Synthetic and Biological Colloids, Ministry of Education, School of Chemical and Material Engineering, Jiangnan University, Wuxi 214122, Jiangsu, China.
Email: wanghj329@outlook.com

Funding information
the MOE & SAFEA for the 111 Project, Grant/Award Number: B13025

Catalytic transfer hydrogenation (CTH) of ethyl levulinate (EL) to γ-valerolactone (GVL) is an alluring reaction in the field of biomass catalytic conversion, but it normally depends on the consumption of H_2. In this study, we report a porous Zr-containing inorganic pyrophosphate catalyst (ZrOPP), which was used as a catalyst for CTH of EL to GVL in the presence of isopropanol and characterized using FT-IR, py-FTIR, TGA, XRD, BET, XPS, ICP-AES, SEM, TEM, NH_3-TPD, and CO_2-TPD. We achieved a high yield of 94% GVL at 433 K for 11 hr. Furthermore, the ZrOPP has the trait of easy separation and could be reused more than five times without distinct decrease in activity and selectivity. In addition, this catalyst could also be applied to other catalytic hydrogenation reactions, such as those of cyclohexanone, acetophenone, 2-heptanone etc. Its outstanding performance was mainly ascribed to the acid sites from the Zr element and basic sites from phosphate groups interspersing on the surface of the catalyst.

KEYWORDS

catalytic transfer hydrogenation, ethyl levulinate, isopropanol, zirconyl pyrophosphate, γ-valerolactone

1 | INTRODUCTION

In the last few years, the growing consumption of fossil resources and alarming environmental pollution have received much attention.[1–3] In addition, biomass is the most abundant and sustainable resource on the earth, and it has been discussed to dispose of the energy crisis and environmental pollution. To date, various value-added chemicals could be acquired from biomass, such as 5-hydroxymethylfurfural (HMF), levulinic acid (LA), γ-valerolactone (GVL), 2,5-dimethyfuran, polyol, and so on.[1,4] Among these chemicals, GVL has been considered to be a versatile chemical that could be used as a liquid fuel, perfume, and food additive. Besides, GVL can be employed not only as a precursor for the production of gasoline and diesel fuels but also as a green solvent for improving biomass conversion in ways of accelerating the initial formation rate of the product and slowing down product degradation.[5]

Nowadays, the catalytic transformation of ethyl levulinate (EL) into GVL is very interesting in the point of view of chemistry. The reaction process is generally considered in such a way: the ketone group on EL is hydrogenated to form hydroxy levulinic ester, which was ring-closed by intramolecular transesterification to produce GVL and the corresponding alcohol.[6] Many homogeneous and heterogeneous catalysts have been used in this process. Yang et al. reported a smart strategy to fabricate Ru nanoparticle-inserted porous carbon, achieving the conversion of LA to GVL with H_2 as a hydrogen source.[7] Furthermore, Banerjee et al. put forward a core–shell nanoreactor storing Pd (0) to produce GVL from EL by decomposing formic acid to offer the

hydrogen source.[8] The special carrier structure is helpful for the loading and dispersion of the metal nanoparticles, promoting the transfer hydrogenation reaction of EL to GVL. Although good yields of GVL were obtained, these hydrogenation methods suffered from high H_2 pressure, the use of precious metals, a low catalyst stability, and the corrodibility of formic acid, which limited their large-scale application.[9] Therefore, it is an ideal task to search for an efficient way to produce GVL.

As we all know, the catalytic transfer hydrogenation (CTH) reactions are a conspicuous alternative to achieve the reduction of carbonyl compounds.[10] The most critical step in the conversion of EL to GVL is the CTH of EL. Many catalysts have been prepared for catalytic hydrogenation of aldehydes and ketones. Mcnerney et al. reported a well-defined monomeric aluminum complex, which could be applied as a general catalyst in the CTH reaction. Perfect catalytic activity is attributed to its unique monomeric nature and the poor coordination of neutral donor isopropanol to the aluminum center.[11] Gawande and coworkers applied the Ag@Ni magnetic core-shell nanocatalyst first to transfer hydrogenation reactions of carbonyl compounds.[12] Wu et al. introduced a chiral *N*,*N*-dioxide/Y(OTf)$_3$ complex to bring about the reduction of glycosylates. It was found that the adjunction of both molecular sieves and Al(OtBu)$_3$ was effective for the reaction.[13] There are many catalysts used in the CTH reaction, but for this kind of reaction there still exist limiting factors, such as a high reaction temperature,[14] a long reaction time,[15] complex operation of the catalyst preparation process, and expensive catalyst materials. Therefore, it is a vital topic for us to look for an efficient, simple, cheap, and general catalyst for this kind of reaction.

There were many reports about connecting phosphate with zirconium to form catalysts.[16–18] But pyrophosphate is different from phosphate. Pyrophosphate possesses a symmetric structure, it could link with zirconium to become a relatively regular structure. Zirconium pyrophosphate (ZrOPP) has a porous structure comprising of a phosphorus oxygen tetrahedron and zirconium atoms. Each phosphorus forms a tetrahedron with four oxygen atoms and shares oxygen atoms with zirconium to accumulate to form a layered structure.[19] Compared with zirconyl pyrophosphate, other Zr-based catalysts have shortcomings in the process of preparation. For example, the synthesis of Zr-Beta requires a longer crystallization time and the preparation of Zr(salphen)-MCM-41 involves a tedious preparation process.[20,21] However, these catalysts play a role in the conversion of LA and its ester. In this study, we firstly introduce zirconium pyrophosphate (ZrOPP) to achieve a series of CTH reactions, especially the conversion of EL to GVL. Its excellent performance is attributed to the interaction between zirconium and oxygen providing the Lewis acid sites and basic sites, respectively. At the same time, ZrOPP is convenient to separate and has high recyclability.

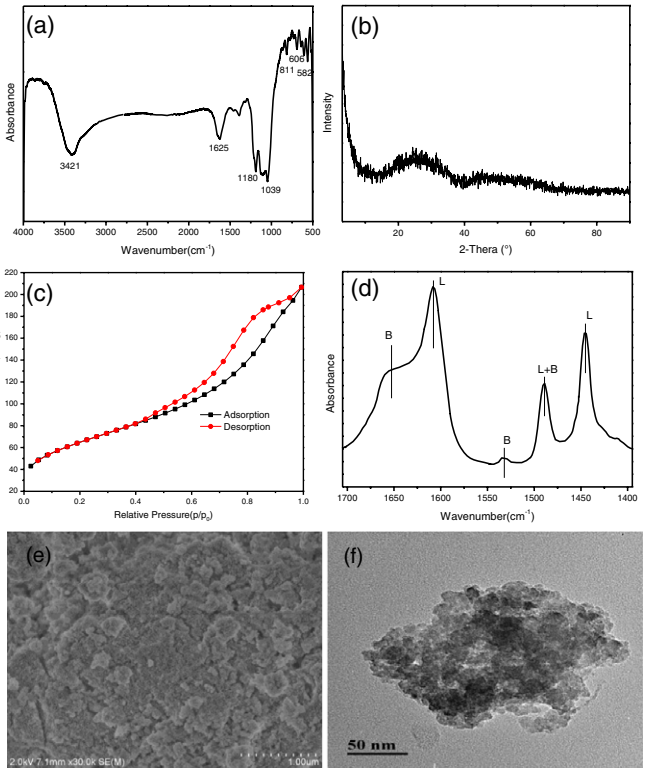

FIGURE 1 Characterization of the prepared ZrOPP. The FT-IR spectra of ZrOPP (a), the powder XRD pattern of ZrOPP (b), the N_2 adsorption–desorption isotherm of ZrOPP (c), pyridine adsorption IR spectra of ZrOPP (d), SEM and TEM images of ZrOPP (e,f)

2 | RESULTS AND DISCUSSION

2.1 | Characterization of catalysts

The Fourier transform-infrared (FT-IR) technique was used to characterize the ZrOPP catalyst (Figure 1a). In each spectrum, there are a strong broad band at 3,421 cm^{-1} and a sharp band at 1,625 cm^{-1} corresponding to the surface-adsorbed water and hydroxyl groups.[22] A weak band at 1,180 cm^{-1} is attributed to the P-O asymmetrical stretching vibration from the $RPO_2(OH)$ groups.[23,24] Besides, the symmetrical stretching modes of the O_3P groups are observed because of the strong absorption at 1,039 cm^{-1},[25] which was attributed to the stretching vibrations of P-O-Zr and could be taken as evidence of the structural formation of zirconium phosphonate.[26] Peaks at 811 and 606–562 cm^{-1} are assigned to the framework vibration of Zr-O-P and Zr-O bonds, respectively.[27,28]

The powder XRD pattern of the synthesized catalyst is shown in Figure 1b. There is no X-ray crystal structure in the XRD pattern. Furthermore, the XRD pattern revealed one broad diffraction peak, enucleating that the synthesized catalyst was amorphous. The textural parameters of the prepared ZrOPP were measured using the N_2 adsorption–desorption method after the sample was degassed at 120 °C for 6 hr. It can be seen that the N_2 adsorption–desorption isotherm of the catalyst exhibits a type IV mode obviously,

showing pore condensation with palpable adsorption–desorption hysteresis (Figure 1c). When p/p_0 was less then 0.4, N_2 was mainly monolayer adsorbed on the surface of ZrOPP. At this time, the adsorption amount of p/p_0 and N_2 was linear. When p/p_0 reached 0.4, the curve entered the jump stage, mainly caused by the capillary condensation of the N_2 molecules in the mesopores. At the same time, it could be found that the N_2 adsorption capacity increased sharply. The mesoporous structure of ZrOPP was well illustrated. In addition, the size and distribution of the pore size were determined by the abrupt position of the capillary condensation. The greater the change rate of the N_2 adsorption and the partial pressure, the more uniform the pore size of the material was. The results illustrated that the material was porous. In addition, the pore volume, the average pore diameter, and the Brunauer–Emmett–Teller (BET) surface area of the catalyst were 0.24 cm^3/g, 6 nm, and 159 m^2/g. To prove the existence of both Lewis acid sites and Brønsted acid sites in the ZrOPP, we also further tested the acid properties using the FT-IR spectra of pyridine adsorption. As shown in Figure 1d, the obvious bands at 1,446 and 1,608 cm^{-1} were assigned to pyridine adsorbed on Lewis acid sites, which confirmed the presence of Lewis acid species chiefly stemming from Zr-O-P and dissociative zirconium ions.[29] In addition, the weak bands at 1,534 and 1,660 cm^{-1} were attributed to pyridine adsorbed on Brønsted acid sites, which testified the existence of Brønsted acid species primarily originating from –OH on the surface of ZrOPP. The peak at 1,489 cm^{-1} belonged to pyridine adsorbed on both Brønsted and Lewis acid sites.[30] These acid sites are favorable for enhancing the catalytic activity and they play different roles in the process of catalytic reaction. Scanning electron microscopy (SEM) and transmission electron microscopy (TEM) demonstrated that the catalyst consisted of conglomerated particles to form a laminated structure and had no uniform shape (Figure 1e,f).

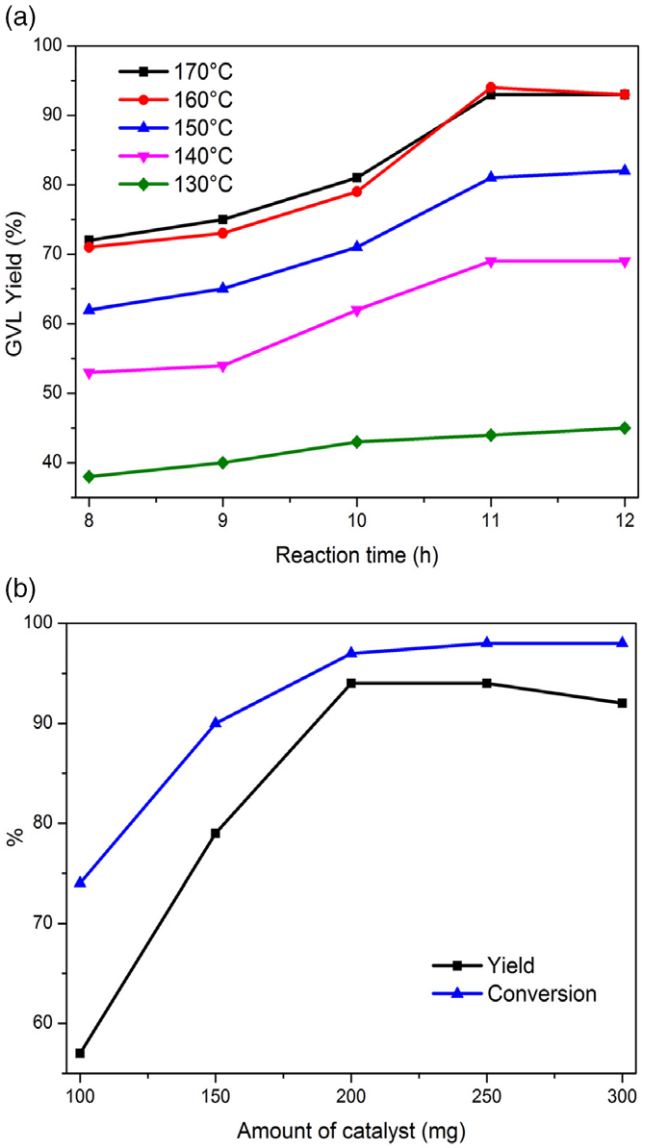

FIGURE 2 Influence of the reaction time and reaction temperature (a). Reaction conditions: EL 1 mmol; isopropanol 5 mL; ZrOPP 200 mg; effect of ZrOPP amount (b). Reaction conditions: EL 1 mmol; isopropanol 5 mL; reaction temperature 160 °C; reaction time 11 hr

2.2 | Influence of different reaction parameters on the reaction

During the reaction process of conversion of EL to GVL. The influence of the reaction time and reaction temperature was discussed to achieve optimal reaction conditions in the presence of 200 mg ZrOPP with isopropanol as a hydrogen source (Figure 2a). In a relatively short reaction time, the yield of GVL and conversion of EL were not high. When the reaction time reached 11 hr, EL was nearly transformed completely and the yield of GVL is up to 94%. After 11 hr, there was no obvious augment in terms of the yield and selectivity of GVL. Meanwhile, with the rise of temperature, the yield and selectivity of GVL were improved, respectively, and remains almost invariant after 160 °C. Therefore, 11 hr and 160 °C were the optimum time and temperature, respectively, for the reaction.

The impact of the amount of ZrOPP on conversion of EL to GVL was discussed at 160 °C with a reaction time of 11 hr and the results are shown in Figure 2b. It could be seen that the yield and selectivity of GVL increased with the incremental amount of the catalyst. At the beginning, the amount of catalyst was 50 mg, and the selectivity of GVL was 46%. The main by-product was ethyl 4-isopropoxylpentanote from GC–MS analysis. 97% conversion of EL and 94% yield of GVL were achieved when the catalyst amount was 200 mg. After that, more amounts of catalyst promoted side reactions, which cut down the yield and selectivity of GVL slightly. In summary, 200 mg was an appropriate amount of catalyst.

2.3 | Reusability and heterogeneity of the catalyst

The reusability of ZrOPP was also examined in the experiment. After each reaction, the catalyst was recovered by

centrifugation and washed with ethyl ether for the next run. As shown in Figure 3a, there was no obvious abatement in the yield and selectivity of GVL after five cycles. Meanwhile, we also explored the leaching of the catalytic species and heterogeneity of the catalyst. After 9 hr of reaction, the catalyst was filtered and the reactor was put back into the oil bath to keep on the reaction. The result is shown in Figure 3b. It was obvious that the yield did not continue to increase after the catalyst filtering, indicating that the active component in the catalyst was not soluble in the reaction system and the reaction proceeded with heterogeneous catalysis. In addition, the thermogravimetric analysis (TGA) showed that the thermogravimetric curve was very steep within 100 °C and then the loss was not obvious (see the ESI). This indicated that the part of loss was because of water and ZrOPP had a good thermal stability. Therefore, the catalyst could be stable at the reaction temperature. Furthermore, the catalyst was characterized using FT-IR, XRD, SEM, and the N_2 adsorption–desorption isotherm (in the ESI) after five cycles. There was no much change in the element content and BET surface area (in the ESI). All of these indicated that ZrOPP was rather stable.

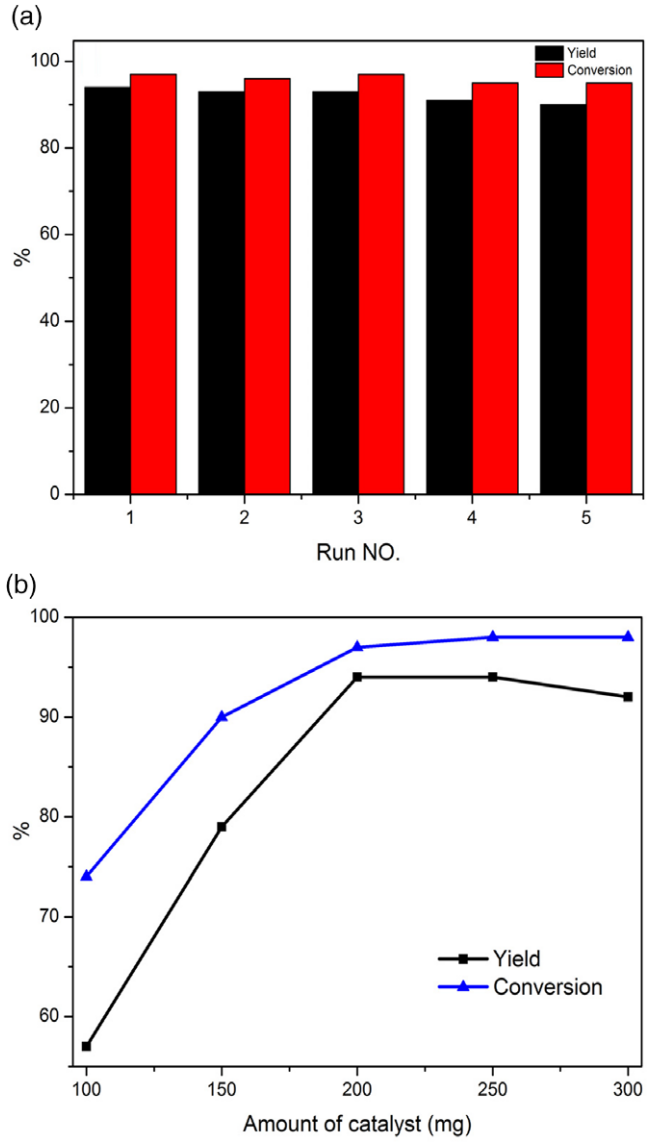

FIGURE 3 Reusability of the catalyst (a). Reaction conditions: EL 1 mmol; isopropanol 5 mL; ZrOPP 200 mg; reaction temperature 160 °C; reaction time 11 hr. Heterogeneity of the catalyst (b). (i) Time-yield plots for CTH reaction of EL catalyzed by ZrOPP. Reaction conditions: EL 1 mmol; isopropanol 5 mL; ZrOPP 200 mg; reaction time 12 hr; reaction temperature 160 °C. (ii) the line shows the GVL yields upon removing the solid catalyst after 9 hr and continued up to 12 hr

2.4 | Catalytic activity analysis

ZrOPP has a similar structure to ZrO_2 of the skeleton (see the ESI). However, ZrOPP showed a much better catalytic activity than ZrO_2, which was attributed to the higher Lewis acidity of ZrOPP.

We analyzed the acidity of ZrOPP and ZrO_2 using the NH3-TPD method (Figure 4a). According to the literature, NH_3 as a smaller molecule compared to pyridine can interact with most of the acidic protons, electron acceptor sites, and hydrogen from neutral or weakly acidic hydroxyls.[31] As shown in Figure 4a, ZrOPP exhibited two peaks at 290 and 525 °C, which were related to the weak Lewis acid sites and Brønsted acid sites. The Lewis acid sites mainly resulted from zirconium and the Brønsted acid sites mostly originated from the hydroxyls in ZrOPP. However, ZrO_2 did not show obvious peaks. Therefore, ZrOPP possessed higher catalytic acidity than ZrO_2. At the same time, XPS examinations suggested that the binding energies of Zr in ZrOPP were higher than in ZrO_2 (Figure 4b). The higher effective charge on the Zr atoms in ZrOPP resulted in a stronger Lewis acidity,[32,33] which was beneficial for the activation of the carbonyl groups in EL improving the reaction activity. In addition, the CO_2-TPD method revealed that ZrOPP had much stronger basicity than ZrO_2 (Figure 4c). The oxygen atoms attaching to phosphate and Zr atoms enhanced the basicity of the catalyst. The higher basicity was conducive to the dissociation of the hydroxyl groups of isopropyl alcohol, and increased the activity of the CTH reaction of EL. Moreover, ZrOPP had a higher BET surface area, a larger pore diameter, and a larger pore volume (in the ESI), which were propitious to increase the diffusion of the reactants to the activity center in ZrOPP and accelerated the reaction process.

2.5 | Mechanism

Through the characterization using NH_3-TPD and CO_2-TPD techniques, we could discover that there are numerous Lewis acid sites and basic sites existing in the catalyst, which are propitious to CTH reactions. The acid sites mainly stemmed from the zirconium atoms and the basic sites mostly originated from oxygen atoms in the pyrophosphate groups. Based on references,[14] the possible mechanism of the CTH reaction has been sorted out in Scheme 1. Firstly, the interaction between acid-basic sites in the catalyst and isopropanol led to dissociation of isopropanol to the corresponding

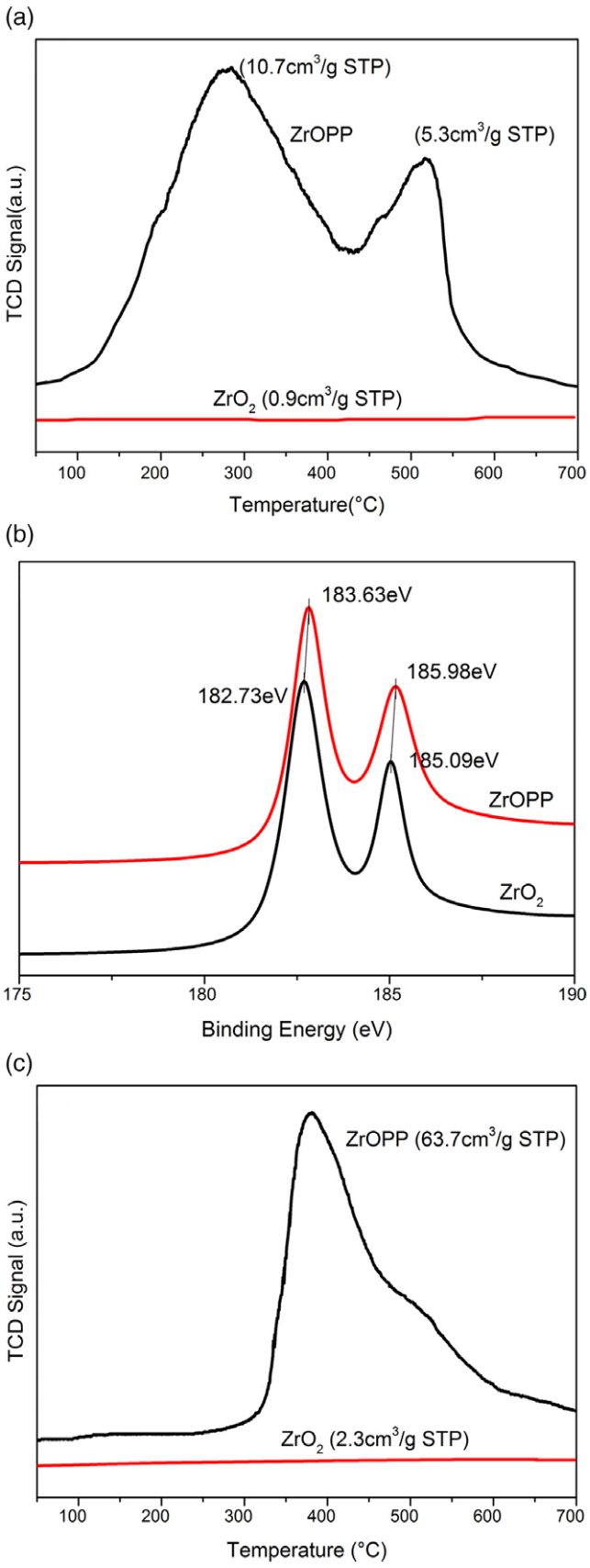

FIGURE 4 NH_3-TPD spectra (a), XPS spectra of Zr 3d (b), and CO_2-TPD spectra (c) of ZrOPP and ZrO_2

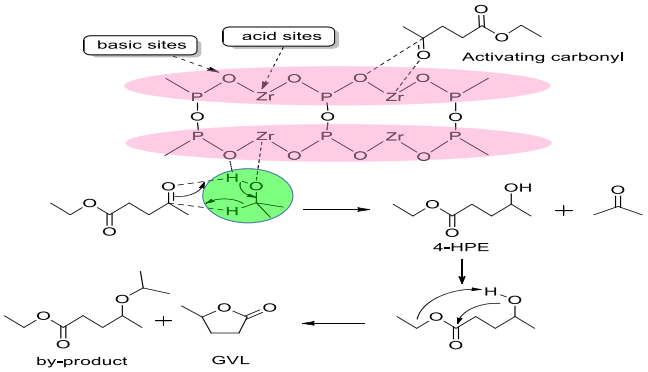

SCHEME 1 The plan of possible mechanism for the transformation of EL to produce GVL catalyzed by ZrOPP via a CTH reaction

alkoxide. Meanwhile, the carbonyl group in EL was activated by acid sites. After that, proton transfer occurred between activated carbonyl and alkoxide to form a six-member intermediate, which further led to produce 4-HPE. Ultimately, 4-PHE was transformed into GVL through an intramolecular transesterification under the boost of acid sites. During the reaction, a part of EL reacted with isopropanol to produce isopropyl levulinate first. Then, the same reaction route occurred and it was similar to EL.

2.6 | Catalytic performance of different catalysts

Many catalysts were applied in the CTH reaction of EL using isopropanol as the hydrogen source and solvent. Different catalysts exhibited distinct catalytic activity and the results are given in Table 1. The reaction did not proceed without catalyst (entry 1). When ZrO_2 was used as the catalyst, the catalytic effect was not satisfying (entry 6). Otherwise, there were many by-products in the process of reaction. Comparatively speaking, $Zr(OH)_4$ and SnO_2/SBA-15 were applied to achieve conversion of EL to GVL in isopropanol, which exhibited a cracking effect (entry 2–3). In addition, Ni/MgO was applied to achieve the conversion of EL with H_2 as the hydrogen source (entry 4). Surprisingly, the reaction proceeded with much higher conversion and selectivity when Al_7Zr_3–300 was used as the catalyst (entry 5). But the reaction conditions are too harsh. In our study, we also synthesized $ZrPO_4$ to use as a catalyst (entry 7). The catalytic effect was better than that of ZrO_2. Then, we prepared ZrOPP as the catalyst acquiring 94% yield of GVL and 97% conversion of EL (entry 8). ZrOPP has a high catalytic activity for the CTH reaction of EL and isopropyl levulinate. Its excellent performance was attributed to the acid sites and basic sites interspersing between the layers in the catalyst, which were conducive to absorb, activate the carbonyl group in EL, and intramolecular esterification ultimately. Furthermore, other hydrogen sources and LA were also used to realize the CTH reaction from EL to GVL with ZrOPP as the catalyst (entry 9–10). As the catalyst was sensitive to the acidity of LA and was not conducive to the reusability of the catalyst, EL was the best choice as the reaction

TABLE 1 CTH reactions of EL in isopropanol catalyzed by different catalysts[a]

Entry	Catalyst	Temp.[b] (°C)	Time (hr)	Con.[c]	Yield	Ref.
1	None	160	11	0	0	—
2	$Zr(OH)_4$	200	1	94	89	[34]
3	SnO_2/SBA-15	110	8	85	81	[35]
4	Ni/MgO	150	2	79	70	[36]
5	Al_7Zr_3-300	220	4	96	83	[37]
6	ZrO_2	160	11	41	14	This work
7	$ZrPO_4$	160	10	72	62	
8	ZrOPP	160	11	97	94	
9[e]	ZrOPP	160	11	97	92	
10[a]	ZrOPP	160	11	92	94	
11	SnOPP	160	11	45	20	
12	TiOPP	160	11	Trace	Trace	

[a] *Reaction conditions*: a stainless reactor of 22 mL; catalyst, 200 mg; EL, 1 mmol; and isopropanol, 5 mL.

[b] Tem. = temperature.

[c] Conversion (Con.) and GVL yield were determined by GC.

[d] The hydrogen donor was 2-butanol.

[e] The reactant was LA.

substrate. In addition, we also prepared other pyrophosphate catalysts, such as SnOPP and TiOPP. However, these two catalysts had little effect on the conversion of EL to GVL (entry 11–12). The amount and strength of acid and basic sites of $ZrPO_4$, SnOPP, and TiOPP were measured using the NH_3-TPD and CO_2-TPD (Figure 5). The amount of NH_3 desorbed from $ZrPO_4$ was much more than that from SnOPP and TiOPP, which was consistent with their catalytic activity. Moreover, the pore volume, average diameter, and BET surface area of $ZrPO_4$, SnOPP, and TiOPP were also analyzed using the N_2 adsorption–desorption method (in the ESI). The BET surface areas of these three catalysts were not large, which was unfavorable for bringing into contact both the catalyst and the reactant sufficiently. However, it could still illustrate that the synergistic effect of phosphate and zirconium played a crucial role in the conversion of the CTH reaction. Moreover, the substitution of pyrophosphate with a symmetrical structure for phosphate not only increased the number of acid and basic sites of the catalyst, but also improved the overall BET surface area, which enhanced the catalytic effect obviously.

2.7 | Catalytic performance of different reactants

As ZrOPP exhibited outstanding activity toward intermolecular hydrogen transfer of EL to GVL, this study was also extrapolated to explore the reactivity of various carbonyl compounds (Table 2). All chosen aldehydes and ketones can be efficiently catalyzed by ZrOPP to produce their corresponding alcohols in high yield. In addition, the reaction conditions of aldehydes are mild compared with ketones (Entry 2, 7). The ketones exhibiting a conjugation effect and possessing a longer carbon chain afford a relatively long reaction time and harsh conditions (Entry 3–8). The higher electron density in the benzene ring results in occupying the Lewis acid centers and reducing the probability of carbonyl groups to contact the active centers. In addition, due to the presence of two benzene rings, the electron cloud density of carbonyl groups on the two phenyl ketones is greatly reduced, which leads to the difficulty of the reaction.

3 | EXPERIMENTAL

3.1 | Materials and methods

Sodium pyrophosphate ($Na_4P_2O_7{\cdot}10H_2O$, AR), Zirconium oxychloride ($ZrOCl_2{\cdot}8H_2O$, AR), isopropanol (AR), isobutanol (AR), naphthalene (AR), LA (98%), furfural (AR), benzaldehyde (AR), acetophenone (AR), cyclohexanone (AR), 2- heptanone (AR), 2- octanone (AR), diphenyl ketone (AR), 4-methyl-2-pentanone (AR), $SnCl_4{\cdot}5H_2O$ (AR), Ti $[SO_4]_2$ (AR), phosphoric acid (85%), and ZrO_2 (AR) were obtained from Sinopharm Chemical Reagent Co. Ltd (Shanghai, China). EL (98%) was gained from Adamas Reagent Co., Ltd. GVL (98%) was purchased from Aladdin Industrial Inc. (Shanghai, China).The SEM images were obtained via a HITACHI S-4800 field-emission scanning electron microscope operated at 15 kV. The TEM was performed on a Jeol JEM model 2,100 microscope operated at 200 kV. FT-IR measurements were recorded on a Nicolet 360 FT-IR instrument (KBr discs) in the wavenumber range of 4,000–500 cm^{-1}. TGA was performed on a STA409 instrument under a nitrogen atmosphere at a heating rate of

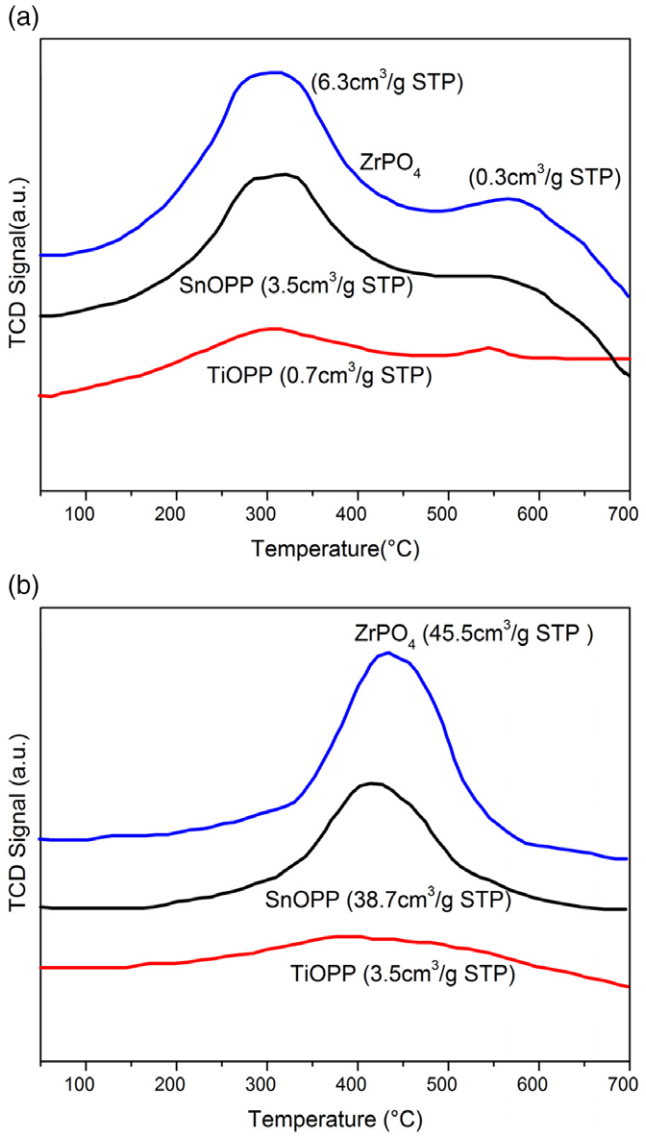

FIGURE 5 NH_3-TPD spectra (a) and CO_2-TPD spectra (b) of $ZrPO_4$, SnOPP, and TiOPP

20 °C/min from 25 to 600 °C. Powder X-ray diffraction (XRD) patterns were collected using a Bruker D8 Advance powder diffractometer (Cu/Kα) in the 2θ range of 10–90° with a scanning speed of 4°/min at 40 kV and 20 mA. The X-ray photoelectron spectra (XPS) were recorded using a Perkin Elmer PHI 5000 ESCT System. The pore volume, pore size, and specific surface area were measured using N_2 adsorption/desorption analysis (Micromeritics ASAP 2020) at 77 K using BET and Barrett–Joyner–Halenda (BJH) methods. The contents of Zr and P in ZrOPP were determined using ICP-AES (VISTA-MPX). The Brønsted and Lewis acid sites of the sample were determined using the FT-IR spectra with pyridine as the probe molecule (Py-FTIR) using a Bruker Tensor 27 spectrometer at 4 cm^{-1} resolution. Prior to analysis, approximately 25 mg of the sample was pressed into a 13 mm self-supported wafer and activated in the IR cell at 673 K for 4.0 hr at 10^{-3} Pa.

TABLE 2 CTH reaction compounds over ZrOPP[a]

Entry	Reactant	Product	Temp. (°C)	*t* (hr)	Conv.[b] (%)	Yield[b] (%)
1			100	4	99	99
2			150	4	99	94
3			140	10	95	90
4			150	10	94	92
5			100	10	95	90
6			100	10	95	95
7			150	11	95	90
8			180	12	Trace	Trace

[a] Reaction conditions: catalyst, 200 mg; reactant, 1 mmol; and isopropanol, 5 mL.

[b] Conversion and yield were determined by gas chromatography (GC).

Following which, it was cooled to room temperature, the sample was exposed to pyridine vapor under vacuum for 0.5 hr followed by evacuation of excess pyridine for 0.5 hr. Then, the cell was heated to 423 K at a rate of 10 K/min and kept at this temperature for 1.0 hr to remove physisorbed pyridine. Temperature-programmed desorption of carbon dioxide (CO_2-TPD) was performed on a Micromeritics' AutoChem1 II 2920 Chemisorption Analyzer. In the experiment, the catalyst was charged into the quartz reactor, and the temperature was increased from room temperature to 300 °C at a rate of 10 °C/min under a flow of He (50 cm^3/min), and then the catalyst was kept at 300 °C for 5 hr. After that, the temperature was decreased to 50 °C. CO_2 (50 cm^3/min) was pulsed into the reactor at 50 °C under a flow of He (10 cm^3/min) until the basic sites were saturated with CO_2. The adsorbed CO_2 was removed by a flow of He (50 cm^3/min). When the baseline was stable, the temperature was increased from 50 to 700 °C at a rate of 10 °C/min. Temperature-programmed desorption of ammonia (NH_3-TPD) was performed on the Micromeritics' AutoChem AutoChem1 II 2920 Chemisorption Analyzer. The catalysts were charged into the quartz reactor, and the temperature was increased from room temperature to 300 °C at a rate of 10 °C/min under a flow of He (50 cm^3/min), and then the catalyst was kept at 300 °C for 5 hr. After that, the temperature was decreased to 50 °C. NH_3/He (10/90, 50 cm^3/min) was pulsed into the reactor at 50 °C under a flow of He (10 cm^3/min) until the acid sites were saturated with NH_3. The adsorbed NH_3 was removed by a flow of He (50 cm^3/min). When the baseline was stable, the temperature was increased from 50 to 700 °C at a rate of 10 °C/min

3.2 | Synthesis of the ZrOPP

In a typical procedure, 1 mmol $Na_4P_2O_7 \cdot 10H_2O$ and 2 mmol $ZrOCl_2 \cdot 8H_2O$ were dissolved in water (25 mL). Then, the

solution of $ZrOCl_2 \cdot 8H_2O$ was added dropwise to the solution of $Na_4P_2O_7 \cdot 10H_2O$ for about 10 min. After that, the mixture was continuously stirred for 10 hr. The white precipitate was separated by filtration, thoroughly washed with H_2O and ethanol to remove Na^+ and Cl^-, and dried at 80 °C for 12 hr, thus the ZrOPP catalyst was obtained. To determine the content of Zr and P by ICP, the ZrOPP was dried at 90 °C for 10 hr. Found: 49.50% Zr, 18.04% P. for $Zr_2P_2O_7$ (356): 51.12% Zr, 17.42% P.

3.3 | Synthesis of the SnOPP and TiOPP

One mmol $Na_4P_2O_7 \cdot 10H_2O$ and 2 mmol $SnCl_4 \cdot 5H_2O$ (or 2 mmol $Ti[SO_4]_2$) were dissolved in water (25 mL). Then, the solution of SnCl4 (or $Ti(SO_4)_2$) was added dropwise to the solution of $Na_4P_2O_7 \cdot 10H_2O$ for about 10 min. After that, the mixture was continuously stirred for 10 hr. The white precipitate was separated by filtration, thoroughly washed with H_2O and ethanol to remove Na^+ and Cl^-(or SO_4^{2-}), and dried at 80 °C for 12 hr, thus SnOPP and TiOPP catalysts were obtained.

3.4 | Synthesis of the $ZrPO_4$

First, a certain amount of $ZrOCl_2 \cdot 8H_2O$ was added in 20 mL of distilled water and sonicated to obtain complete dissolution, afterward H_3PO_4 (85%) was added dropwise for 10 min and sonicated to react. When the reaction was completed, a dispersed white precipitate was obtained. The solid was filtered and washed with distilled water and ethanol several times. Subsequently, the catalyst was dried at 80 °C for 12 hr and calcined at 500 °C for 1 hr to obtain pure $ZrPO_4$.

3.5 | Catalytic reactions

In a typical experiment, EL (1 mmol), isopropanol (5 mL), and the catalyst (200 mg) were charged into a stainless reactor of 22 mL equipped with a magnetic stirrer. After sealing, the reaction mixture was stirred at a known temperature for the desired time. Afterward, the products were analyzed quantitatively by gas chromatography (GC 9700) using naphthalene as the internal standard, and the identification of the products was done by GC–MS (SCIONSQ-456-GC). The yield of GVL was calculated using the following equation:

$$\text{GVL yield (mol\%)} = \frac{\text{Moles of GVL formed}}{\text{Moles of EL used}} \times 100\%.$$

3.6 | Reusability of the ZrOPP

In the experiments to test the reusability of the ZrOPP, the catalyst was recovered by centrifugation, and washed with ethyl ether (3 × 50 mL). After drying under vacuum at 80 °C for 12 hr, the catalyst was reused for the next run.

4 | CONCLUSIONS

In summary, a porous inorganic Zr-containing catalyst (ZrOPP) was prepared and applied to the CTH reaction with isopropanol as the hydrogen source. ZrOPP exhibited very high activity and selectivity for CTH of various carbonyl compounds, especially for the conversion of EL to GVL, which was ascribed to the acidic and basic sites interspersing in the catalyst. In addition, the catalyst can be reused at least five times without losing activity and selectivity. We believe that this highly effective and easy to prepare catalyst has great promise for application in CTH reactions, and the structures similar to that of ZrOPP can also be used to design more and better catalysts

ACKNOWLEDGMENTS

This work was financially supported by the MOE & SAFEA for the 111 Project (B13025).

ORCID

Haijun Wang http://orcid.org/0000-0003-2857-5861

REFERENCES

[1] J. L. Song, L. Q. Wu, B. W. Zhou, *Green Chem.* **2015**, *17*, 1623.
[2] L. K. Ren, L. F. Zhu, T. Qi, *ACS Catal.* **2017**, *7*, 2199.
[3] R. F. Ma, X. P. Wu, T. Tong, *ACS Catal.* **2016**, *6*, 2035.
[4] M. Al-Naji, A. Yepez, A. M. Balu, *J. Mol. Catal. A Chem.* **2016**, *417*, 145.
[5] H. Li, Z. Fang, S. Yang, *ACS Sustain. Chem. Eng.* **2016**, *4*, 236.
[6] D. M. Alonso, S. G. Wettstein, J. A. Dumesic, *Green Chem.* **2013**, *15*, 584.
[7] Y. Yang, C. J. Sun, D. E. Brown, L. Q. Zhang, F. Yang, H. R. Zhao, *Green Chem* **2016**, *18*, 12.
[8] R. Singuru, B. Banerjee, S. K. Kundu, K. Dhanalaxmi, *Catal. Sci. Technol.* **2016**, *6*, 5102.
[9] A. M. Hengne, B. S. Kadu, *RSC Adv.* **2016**, *6*, 59753.
[10] J. R. Ruiz, C. J. Sanchidnan, *Curr. Org. Chem.* **2007**, *11*, 1113.
[11] B. McNerney, B. Whittlesey, D. B. Cordes, C. Krempner, *Chem. Eur. J.* **2014**, *20*, 14959.
[12] M. B. Gawande, H. Z. Guo, A. K. Rathi, P. S. Branco, Y. Z. Chen, R. S. Varma, *RSC Adv.* **2013**, *3*, 1050.
[13] W. B. Wu, S. J. Zou, L. L. Lin, J. Ji, Y. H. Zhang, B. W. Ma, X. H. Liu, X. M. Feng, *Chem. Commun.* **2017**, *53*, 3232.
[14] X. Tang, L. Hu, Y. Sun, G. Zhao, W. Hao, L. Lin, *RSC Adv.* **2013**, *3*, 10277.
[15] M. Chia, J. A. Dumesic, *Chem. Commun.* **2011**, *47*, 12233.
[16] J. Safaei-Ghomi, H. Shahbazi-Alavi, R. Teymuri, *Polycyclic Aromat. Compd.* **2016**, *36*, 834.
[17] F. K. Li, L. J. France, Z. Cai, *Appl. Catal. B Environ.* **2017**, *214*, 67.
[18] J. J. Wang, R. Y. Wang, H. M. Zi, *J. Chin. Chem. Soc.* **2018**.
[19] Z. P. Zhu, T. Y. Ma, Y. L. Liu, T. Z. Ren, Z. Y. Yuan, *Inorg. Chem. Front.* **2014**, *1*, 360.
[20] J. Wang, S. Jaenicke, G. K. Chuah, *RSC Adv.* **2014**, *4*, 13481.
[21] R. Y. Wang, J. J. Wang, *Mol. Catal.* **2017**, *441*, 168.
[22] T. Z. Ren, Z. Y. Yuan, *Chem. Phys. Lett.* **2003**, *374*, 170.
[23] E. V. Bakhmutova-Albert, N. Bestaoui, V. I. Bakhmutov, A. Clearfield, A. V. Rodriguez, *Inorg. Chem.* **2004**, *43*, 1264.
[24] F. Odobel, B. Bujoli, D. Massiot, *Chem. Mater.* **2001**, *13*, 163.
[25] C. Jacopin, M. Sawicki, G. Plancque, D. Doizi, F. Taran, E. Ansoborlo, B. Amekraz, C. Moulin, *Inorg. Chem.* **2003**, *42*, 5015.
[26] Y. Jia, Y. Zhang, R. Wang, J. Yi, X. Feng, Q. Xu, *Ind. Eng. Chem. Res.* **2012**, *51*, 12266.
[27] J. D. Kim, T. Mori, I. Honma, *J. Power Sources* **2007**, *172*, 694.
[28] J. D. Kim, T. Mori, I. Honma, *J. Electrochem. Soc.* **2006**, *153*, A508.

[29] V. V. Ordomsky, J. C. Schouten, T. A. Nijhuis, *Chem Sus Chem.* **2012**, *5*, 1812.
[30] J. José, M. Pedro, O. Pascual, D. J. Jones, R. Jacques, *Adv. Mater.* **1998**, *10*, 812.
[31] J. Ni, L. Chen, J. Lin, S. Kawi, *Nano Energy* **2012**, *1*, 674.
[32] J. L. Song, B. W. Zhou, H. C. Zhou, L. Q. Wu, Q. L. Meng, Z. M. Liu, B. X. Han, *Angew. Chem. Int. Ed.* **2015**, *54*, 9399.
[33] B. Tang, W. Dai, X. Sun, G. Wu, N. Guan, M. Hunger, L. Li, *Green Chem.* **2015**, *17*, 1744.
[34] X. Tang, H. Chen, L. Hu, W. Hao, Y. Sun, X. Zeng, L. Lin, S. Liu, *Appl. Catal. B Environ.* **2014**, *147*, 827.
[35] S. D. Xu, D. Q. Yu, T. Ye, P. P. Tian, *RSC Adv.* **2017**, *7*, 1026.
[36] J. Lv, Z. Rong, Y. Wang, J. Xiu, Y. Wang, J. Qu, *RSC Adv.* **2015**, *5*, 72037.
[37] J. He, H. Li, Y. M. Lu, Y. X. Liu, Z. B. Wu, D. Y. Hu, S. Yang, *Appl. Catal. A Gen.* **2016**, *510*, 11.

SUPPORTING INFORMATION

Additional supporting information may be found online in the Supporting Information section at the end of the article.

How to cite this article: Wang J, Wang R, Zi H, Wang H, Xia Y, Liu X. A porous inorganic zirconyl pyrophosphate as an efficient catalyst for the catalytic transfer hydrogenation of ethyl levulinate to γ-valerolactone. *J Chin Chem Soc*. 2018;1–9. https://doi.org/10.1002/jccs.201800073